Nano Energy 112 (2023) 108464

Contents lists available at ScienceDirect

Nano Energy

journal homepage: www.elsevier.com/locate/nanoen

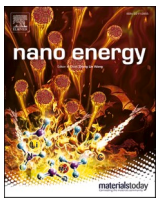

The process of free radical generation in contact electrification at solid-liquid interface☆

Yi Zhao [a,b,e], Yang Liu [a], Yuying Wang [a], Shulan Li [c], Yi Liu [a,c,*], Zhong Lin Wang [d,**], Peng Jiang [a,b,e,*]

[a] College of Chemistry and Molecular Sciences & School of Pharmaceutical Sciences & Department of Orthopedics Trauma and Microsurgery (Zhongnan Hospital of Wuhan University), Wuhan University, Wuhan 430072, P.R. China
[b] Key Laboratory of Combinatorial Biosynthesis and Drug Discovery (MOE), Wuhan University, Wuhan 430071, P.R. China
[c] State Key Laboratory of Separation Membrane and Membrane Process & Tianjin Key Laboratory of Green Chemical Technology and Process Engineering, School of Chemistry and Chemical Engineering, Tiangong University, Tianjin 300387, P.R. China
[d] Beijing Institute of Nanoenergy and Nanosystems, Chinese Academy of Sciences, Beijing 100083, China
[e] Hubei Jiangxia Laboratory, Wuhan 430200, P.R. China

ARTICLE INFO

Keywords:
Solid-liquid interfaces
Electron transfer
Hydroxyl radical
Superoxide anion radical

ABSTRACT

Solid-liquid interfaces are ubiquitous in nature and widely used in various applications such as catalysis, sensing, batteries, etc. Recently, we found the existence of electron transfer at the interface in solid-liquid contacting, and proposed a "two-step" theory for the formation of solid-liquid electric double layer (EDL). In this work, we found that hydroxyl radical (·OH) was generated when the droplet contact with the tube inner wall without external interference, and the concentration of·OH was increased with increasing pH, demonstrating that the·OH was generated from hydroxide ions (OH^-) by electron transfer during contact electrification. This can be further supported by the fact that capillaries made of materials with stronger electron-withdrawing ability could generate more·OH. Interestingly, superoxide anion radical ($\cdot O_2^-$) was not generated at the solid-liquid interface if no external energy is provided. However, if ultrasonic was applied,$\cdot O_2^-$ could be generated at the solid-liquid interface, because ultrasonication provides transition energy for the electron to transfer from the solid to O_2 at the interface. Based on the generation of reactive oxygen species (·OH and$\cdot O_2^-$), we demonstrated a proof-of-concept for degradation of tetracycline pollution. This work provides an excellent strategy to study the solid-liquid interface and also provides a new insight into the free radical generation at the interface in solid-liquid contacting.

1. Introduction

Solid-liquid interfaces are ubiquitous in nature and widely used in various applications, such as catalysis [1–3], sensing [4–7], batteries [8,9], etc. For instance, in non-homogeneous catalytic reactions, the activity of the catalytic reaction and the state of the catalyst can be reflected in real time by detecting the chemical currents generated at the solid-liquid interface [10]. Apart from that, the properties of solid-liquid interface can affect the electrochemical reaction, especially the properties of the electric double layer (EDL) [11], which is decisive in extending the battery life. Therefore, exploring the intrinsic interfacial reactions present in solid-liquid contact can provide new insights into these applications.

Recently, Lee et al. reported that H_2O_2 could be spontaneously produced in water microdroplets formed by dropwise condensation of water vapor on low temperature solid surfaces, such as Si surface [12]. However, the H_2O_2 generation mechanism has not been investigated. In fact, there is a continuous solid-liquid contact process during the

☆ Prof Zhong Lin Wang, an author on this paper, is the Editor-in-Chief of Nano Energy, but he had no involvement in the peer review process used to assess this work submitted to Nano Energy. This paper was assessed and the corresponding peer review managed by Professor Chenguo Hu, also an Associate Editor in Nano Energy.

* Corresponding authors at: College of Chemistry and Molecular Sciences & School of Pharmaceutical Sciences & Department of Orthopedics Trauma and Microsurgery (Zhongnan Hospital of Wuhan University), Wuhan University, Wuhan 430072, P.R. China.
** Corresponding author.
E-mail addresses: yiliuchem@whu.edu.cn (Y. Liu), zhong.wang@mse.gatech.edu (Z.L. Wang), jiangpeng@whu.edu.cn (P. Jiang).

https://doi.org/10.1016/j.nanoen.2023.108464
Received 14 March 2023; Received in revised form 7 April 2023; Accepted 18 April 2023
Available online 20 April 2023

condensation process. So, we speculate that there is a solid-liquid interfacial reaction in the condensation process leads to the generation of H_2O_2. Previously, we reported that electron transfer is the main mechanism of contact electrification between solid-solid pairs [13–16]. Then we extended this mechanism to the solid-liquid interface and proposed a "two-step" theory for the formation of solid-liquid EDL [17], that is, electron transfer occurs instantaneously when the liquid comes in contact with the original solid surface (step 1), followed by the adsorption of counter ions (step 2). This theory was confirmed by the decay of contact electrification charges on the solid surfaces after liquid-solid contact electrification at different thermal conditions [18]. Moreover, the study of contact electrification process between different liquids and polytetrafluoroethylene (PTFE) film demonstrated that electron transfer plays the dominant role during contact electrification between liquids and solids [19]. More recently, we successfully detected hydroxyl radical (·OH) and superoxide anion radical ($\cdot O_2^-$) using Fluorinated ethylene propylene (FEP) powder with the assistance of ultrasonication, confirming that the electron transfer caused by the contact electrification of solid-liquid contact can induce a solid-liquid interfacial reaction to produce reactive oxygen species (ROS) [20]. However, ultrasonic is a high-energy source, the use of ultrasonic may interfere with the electron transfer process and the interfacial reactions that generated ROS [21,22]. Therefore, there remains a need for directly studying the interfacial reactions induced by electron transfer during solid-liquid contact.

Herein, we propose a highly sensitive strategy for investigating the electron transfer and free radical generation during solid-liquid contact. In this strategy, a small droplet was pushed through a long capillary tube by nitrogen gas flow to provide continuative solid-liquid contact, which can generate a sufficiently high concentration of free radical in the small droplet without the assistance of ultrasonication. Our results demonstrated that the generated free radical without ultrasonic are·OH, which is formed from the hydroxide ion (OH^-) by losing one electron during contact electrification at the solid-liquid interface. Notably,$\cdot O_2^-$ was not detected in the solid-liquid contact process. However,$\cdot O_2^-$ can be obviously detected with the introduction of ultrasonic, confirming that the use of ultrasonic indeed interfere with the electron transfer process and the interfacial reactions. Moreover, the concentration of·OH also significantly increased with the assistance of ultrasonication. Furthermore, the ultrasonic-assisted free radical generation could be used to degrade tetracycline pollution.

2. Experimental section

2.1. Chemicals and materials

O-phenylenediamine (OPD, $C_6H_8N_2$, Sinopharm Chemical Reagent Co., Ltd, ≥98%), 3,3′,5,5′-tetramethylbenzidine (TMB, $C16H_{20}N_2$, Anegis, 98%), terephthalic acid (TA, $C_8H_6O_4$, Sinopharm Chemical Reagent Co., Ltd, 99%), Dihydroethidium (DHE, $C_{21}H_{21}N_3$, Aladdin, 95%), Tert-butanol ($C_4H_{10}O$, Maclean, 99.5%), 1,4-Benzoquinone ($C_6H_4O_2$, Aladdin, 99%), methylene blue ($C_{16}H_{18}ClN_3S$, Sinopharm Chemical Reagent Co., Ltd, ≥98%). Tetracycline hydrochloride ($C_{22}H_{24}N_2O_8$·HCl, Aladdin, 96%), Polytetrafluoroethylene (PTFE), Food-grade high-temperature silicone rubber (Silicone Rubber) and Cast nylon 6 (Nylon 6) were purchased from Shanghai Daoguan Company. All chemical reagents used in this study were of analytical grade and could be used directly without further purification. The experimental water was deionized water (18.2 MΩ cm^{-1}) purified by Millipore systemin the whole process.

2.2. Characterization

The absorption spectra were characterized by the Cary series ultraviolet-visible absorption spectrometer (Agilent Technologies, USA). The tetracycline absorption spectra were characterized by the double-beam UV-Vis spectrophotometer (TU-1900, China). The fluorescence spectra were measured using the Cary Eclipse fluorescence spectrometer (Agilent Technologies, USA). ESR spectra was obtained by the electron paramagnetic resonance (EPR) spectrometer (Bruker A300, Germany). Degradation of tetracycline at different time intervals was recorded by electrospray ionization mass spectrometry (ESI-MS) on an Agilent quadrupole time-of-flight high-resolution liquid mass spectrometer (Q-TOF LC-MS) with the ion source of the mass spectrometer set to positive ion mode (Agilent Technologies, USA). The injection volume was 6 μL, the mobile phase consisted of 16% acetonitrile and 84% formic acid solution.

3. Results and discussion

3.1. Generation of hydroxyl radical induced by contact electrification at solid-liquid interface

The experimental setup is shown in Fig. 1a and b, a small water droplet (135 μL) was injected into the capillary tube through a syringe (Step 1) and then pushed it through a long capillary tube by nitrogen gas flow, and the liquid was collected at the end of the capillary tube for subsequent free radical detection (Step 2). This setup has the following advantages: (1) it can produce a large solid-liquid contact interface for a small volume of water, thereby increasing the free radical concentration generated by solid-liquid interface contacting; (2) the free radical concentration can be further increased by extending the tube length; (3) the nitrogen atmosphere can eliminate oxygen interference.

According to the reported studies, the contact electrification process could be significant affected by the difference in electron-withdrawing ability of the two contact materials, that is greater differences can drive more electron transfer [23]. In order to investigate the contact electrification-induced free radical generation at solid-liquid interface, three frictional materials with different electron-withdrawing ability were selected as solid layers in our experiments, namely: PTFE, Silicone Rubber and Nylon 6. The electron-withdrawing ability order of these three materials is: PTFE > Silicone Rubber > Nylon 6 [24]. Here, 1, 2-diaminobenzene (OPD) was used as a detection probe for·OH, the detection mechanism is that OPD can be oxidized by·OH to produce diaminophenothiazine (DAP) with maximum absorption at 424 nm (Fig. 1c). Fig. 1d shows the UV–vis absorption spectra of OPD solutions treated with PTFE, Silicone Rubber and Nylon 6 under identical conditions (the length is 5 m), respectively. A control group was carried out under identical conditions without passing through capillary tube. As shown in Fig. 1d, the characteristic absorption spectra corresponding to DAP did not appeared in control group, but appeared in the three experimental groups, indicating that·OH was produced when water contact with all these three materials, and the·OH concentration is consistent with electron-withdrawing ability, that is: $[\cdot OH]_{(PTFE)} > [\cdot OH]_{(Silicone\ Rubber)} > [\cdot OH]_{(Nylon\ 6)}$. The generation of·OH could be further confirmed by the 1:2:2:1 characteristic peaks corresponding to the DMPO-·OH adduct in the electron spin paramagnetic resonance (ESR) spectra (Fig. S1). The·OH generation in PTFE tube with different length (0 m, 1.5 m, 7.5 m and 15 m) show that the·OH concentration is increased with PTFE tube length, which is attributed to the increased solid-liquid contact interface (Fig. 1e and Fig. S2).

Du et al. reported that·OH readily combine to form H_2O_2 in the presence of water [25]. Therefore, the H_2O_2 level in the water collected at the end of the capillary tube was measured to further confirm the·OH generation. In this experiment, 135 μL of deionized water flowed through 15 m PTFE tube, and the H_2O_2 level of the collected water was measured using 3,3′,5,5′-tetramethylbenzidine (TMB), which appeared a characteristic absorption peak at 652 nm after oxidized by H_2O_2. The results show that the H_2O_2 concentration in PTFE tube treated group is much higher than that of control group (Fig. 1 f and Fig. S3), further confirming the·OH generation. Fig. 1 g and Fig. S4 shows the effect of ion concentration in solution on·OH generation, the amount of·OH

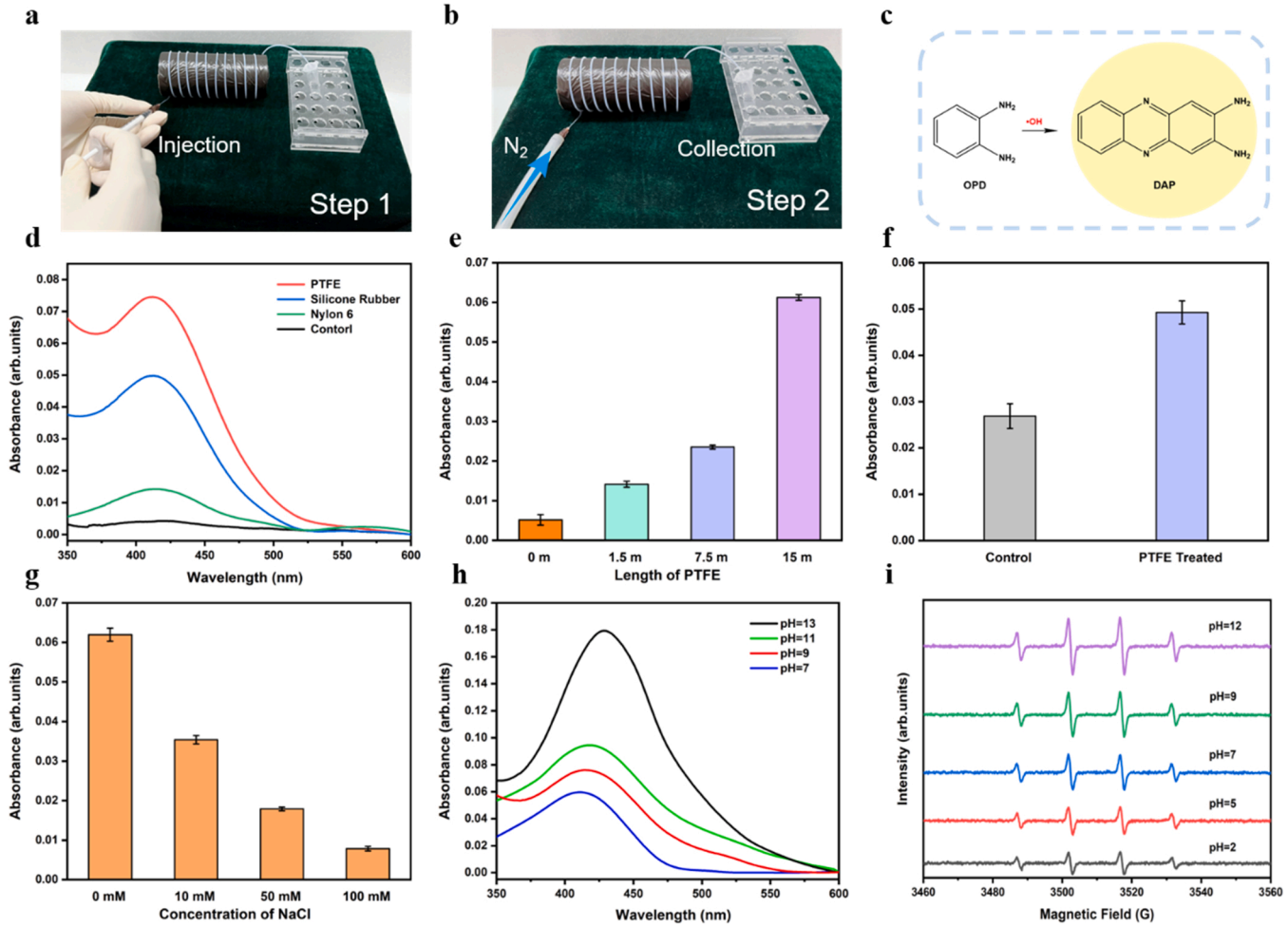

Fig. 1. Generation of·OH induced by contact electrification at solid-liquid interface. (a, b) Photographs of the experimental setup. (c)·OH detection mechanism of OPD. (d) Absorption spectra of OPD solution treated with different capillary tube materials (PTFE, Silicone Rubber, Nylon 6). (e) Maximum absorption of OPD solution treated with different PTFE capillary tube lengths. (f) Maximum absorption of TMB solution (10 mg mL^{-1}) treated and untreated with PTFE capillary tube. (g) Maximum absorption of PTFE-treated OPD solution with different concentrations of NaCl. (h) Absorption spectra of OPD solution treated with PTFE capillary tube at different pH. (i) DMPO-·OH electron spin paramagnetic resonance (ESR) spectra of PTFE-treated solution at different pH. Error bars represent standard deviation based on three replicate data.

decreases as the NaCl concentration increases (0 mM, 10 mM, 50 mM, 100 mM). This phenomenon is attributed to the shielding effect, which can hinder the electron transfer process, and ultimately affecting the production of·OH [19,26].

To elucidate the·OH generation mechanism, the effect of pH was investigated. As shown in Fig. 1 h and i, the·OH concentration gradually increases as the pH of OPD solution increase from 7 to 13. The ESR results at different pH conditions also showed the same trend. Based on the above results, it can be concluded that·OH was generated from hydroxide ions (OH^-) in water by losing one electron when it contacted with solid layer such as PTFE.

3.2. Generation of·OH and·O_2^- at the solid-liquid interface with ultrasonic

In our previous work, both·OH and·O_2^- could be produced using FEP powder in water with the assistance of ultrasonication. However, the above results in this work have confirmed that only·OH was generated and·O_2^- was not detected in the solid-liquid contact process, suggesting that ultrasonic may affect the free radical production. To examine the effect of ultrasonic on free radical production, ultrasonic was applied in the following experiments. Here, a 25 cm tube filled with aqueous liquid was placed in a ultrasonicator, and then the ultrasonic-treated solution was collected for the following measurement. The absorption spectra of DAP in Fig. 2a show that the introduction of ultrasonic promoted the·OH production. This can be further confirmed by the ESR results in Fig. 2b. Then, the effect of capillary material, thickness of capillary wall and pH of liquid on·OH generation was investigated. Terephthalic acid (TA) was used as detection reagent for·OH, the detection mechanism is that TA can be oxidized by·OH to produce TA-OH with fluorescence emission at 425 nm. Fig. 2c shows the fluorescence spectra of TA solutions treated with PTFE, Silicone Rubber and Nylon 6, respectively, which shows the same trend with the above results obtained without the ultrasonic as shown in Fig. 1d. In addition, the effect of thickness of capillary wall was investigated. Fig. 2d shows the·OH generation in capillary tube with three different wall thickness (inner*outer diameter: 1 *1.4 mm, 1 *2 mm, 1 *3 mm). It is evident from Fig. 2d and Fig. S5 that thinner capillary walls are more conducive to the utilization of ultrasonic energy, correspondingly, produce more·OH. Furthermore, the generation of·OH under different pH was also measured using TA assay. As shown in Fig. 2e, the·OH concentration gradually increases as the pH of TA solution increases, which is consistent with the above results in Fig. 1 h. These results indicated that the·OH generation by contact electrification at the solid-liquid interface also occurs under ultrasonication, and ultrasonic could promote the·OH generation.

To investigate whether·O_2^- generated under ultrasonication, ESR spectra was also performed. Here, methanol was added to quench

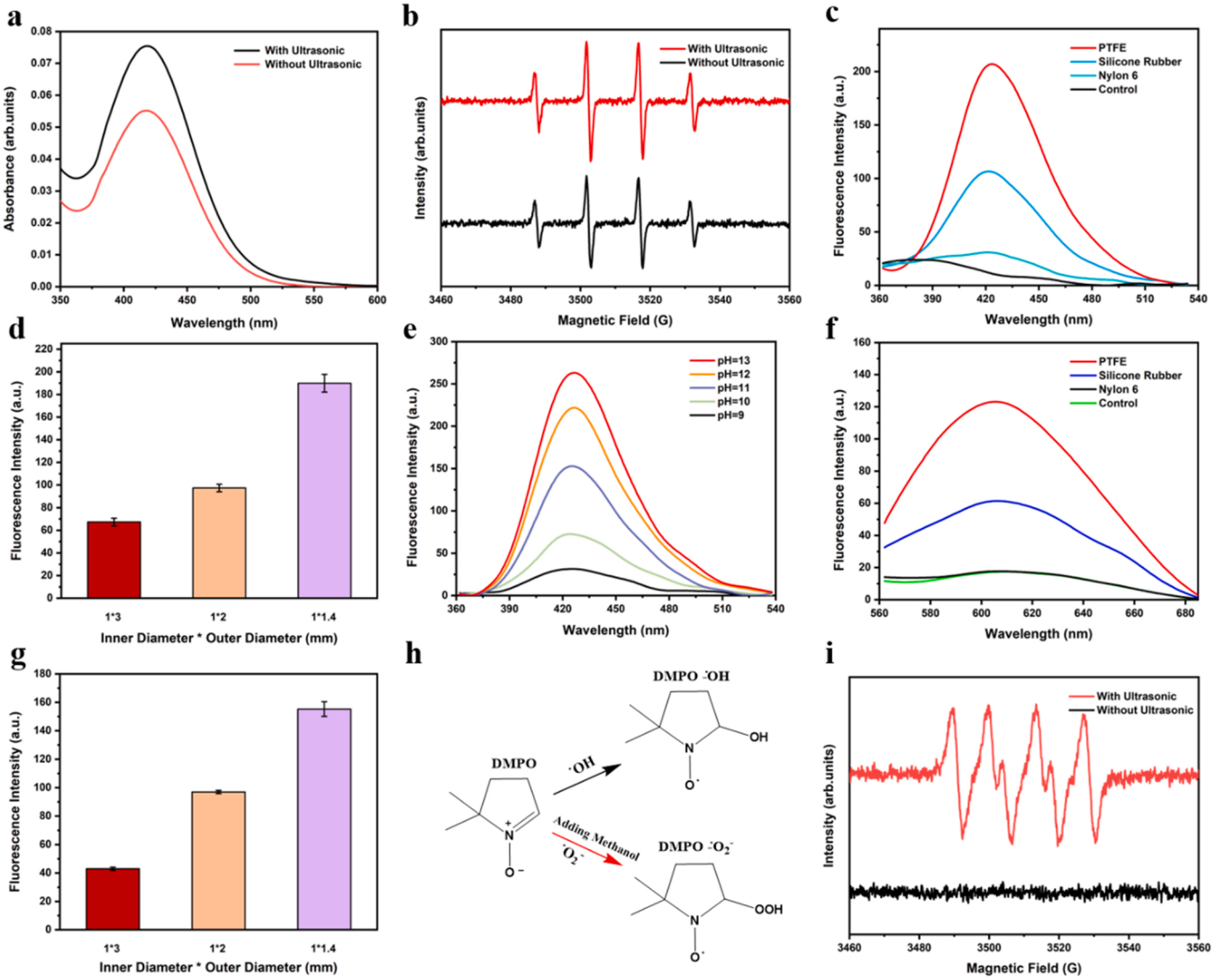

Fig. 2. Effect of ultrasonic introduction on radical generation during CE. (a) Absorption spectra of PTFE-treated OPD solution with or without ultrasonic. (b) DMPO-·OH ESR spectra of PTFE-treated solution with or without ultrasonic. (c) Fluorescence spectra of TA solution treated with different capillary tube materials (PTFE, Silicone Rubber, Nylon 6). (d) Fluorescence intensity of PTFE-treated TA solution with different tube wall thickness (inner diameter*outer diameter: 1 *3 mm, 1 *2 mm, 1 *1.4 mm). (e) Fluorescence spectra of TA solution treated with PTFE capillary tube at different pH. (f) Fluorescence spectra of DHE solution treated with different capillary tube materials (PTFE, Silicone Rubber, Nylon 6). (g) Fluorescence intensity of PTFE-treated DHE solution with different tube wall thickness (inner diameter*outer diameter: 1 *3 mm, 1 *2 mm, 1 *1.4 mm). (h) Schematic diagram of radical capture by DMPO under different conditions. (i) DMPO-·O_2^- ESR spectra of PTFE-treated solution with or without ultrasonic. Error bars represent standard deviation based on three replicate data.

the·OH radical, increasing the chance of the·O_2^- reacting with DMPO, as illustrated in Fig. 2 h. As shown in Fig. 2i, ESR peaks corresponding to·O_2^- are obviously appeared in the ultrasonic-treated group (red line), while no visible peaks of·O_2^- appeared in the non-sonicated group. In addition, Dihydroethidium (DHE), a commonly used fluorescent detection probe for·O_2^- was also used to investigate the·O_2^- generation. DHE can dehydrogenates to ethidium bromide with a maximum emission at 610 nm in the presence of·O_2^-. Fig. 2 f and 2 g show the effect of capillary material and thickness of capillary wall on·O_2^- generation with the assistance of ultrasonication. The results indicated that the most·O_2^- was generated in the PTFE solid layer and more·O_2^- was generated at a thinner capillary wall (Fig. S6).

The above results suggesting that the use of ultrasonic indeed interfere with the electron transfer process and the interfacial reactions in solid-liquid contact process, which may provide the energy via phonon excitation that assistant the release of the electron from solid surface back to the liquid. That is, only·OH can be produced without ultrasonic, while both·OH and·O_2^- can be produced with the assistance of ultrasonication.

3.3. *Mechanism of free radical generation induced by solid-liquid contact electrification*

Based on the above results, we propose the mechanism that induces the generation of free radical during contact electrification (Fig. 3). First, a sufficient solid-liquid contact occurs between the liquid and the long capillary wall driven by nitrogen gas. Due to the stronger electronegativity of PTFE than water, an electron is transferred from OH^- to the PTFE surface upon contact, and the PTFE gains an electron to be negatively charged, while OH^- in solution loses an electron to generate·OH radicals. The free hydrogen ions may be partly combined with water molecules to form hydrated hydrogen ions, and partly transferred to the solid surface due to electrostatic interactions. In addition, the liquid will undergo acoustic cavitation under ultrasonic conditions, and vacuum bubbles will be formed. The collapse of the vacuum bubble results in transient oscillations that further provide more contact points at the

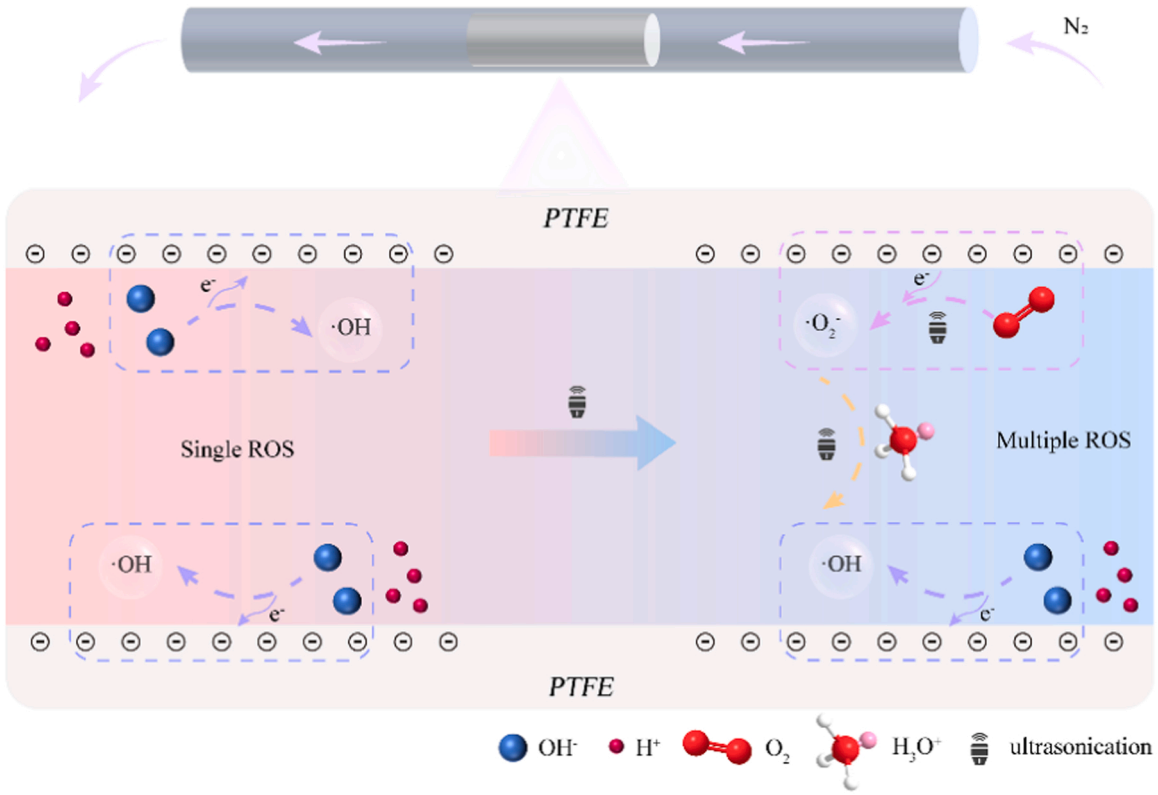

Fig. 3. Mechanism of free radical generation by contact electrification process. The electron transfer from liquid to solid is due to the lower energy state in the solid, which occurs naturally once the two contacts. The sonic wave excitation may provide the energy required for releasing the transferred electron due to the energy provided via phonon.

solid-liquid interface. It also provides the opportunity for the oxygen molecules in the solution to come into contact with PTFE surface. Under the action of ultrasonic, oxygen molecules are released, and grabs the electron from PTFE layer to be reduced to·O_2^-. At the same time, PTFE returns to its uncharged state, ready for the electron transfer for the next solid-liquid contact. In addition, the free water and hydrogen ions may react with the superoxide anion radical by a chain reaction under the action of ultrasonic to produce additional·OH radicals [27].

3.4. Tetracycline degradation application

Tetracycline antibiotics are widely used in clinical and prophylactic applications in humans and animals because of their broad-spectrum antimicrobial properties and good therapeutic effects [28,29]. However, they are so difficult to degrade in the environment that they are deposited in large quantities in soil and water environments [30–32]. These antibiotic-like substances can accumulate excessively through the food chain thus posing a great threat to human public health. In this situation, research on simple and effective strategy to reduce tetracycline contamination is necessary. In this work,·OH and·O_2^- radical induced by solid-liquid contact electrification process were used to degrade tetracycline (as illustrated in Fig. S7). The degradation of tetracycline can be measured by the absorption peak located at 357 nm. First, the degradation ability of the three frictional electric materials used above was evaluated by treating tetracycline (20 μg mL^{-1}) with the assistance of ultrasonication for 60 min. As shown in Fig. 4a, the absorption spectra of all the three materials (PTFE, Silicone Rubber and Nylon 6) can degrade tetracycline. Among them, the degradation efficiency of PTFE is the highest, which consistent with the results of free radical generation. The effect of thickness of capillary wall on the degradation of tetracycline was also studied, and the best degradation efficiency was obtained in the group of 1 * 1.4 mm (Fig. 4b), which also consistent with the trend of free radical generation in Fig. 2d and g. Therefore, a PTFE tube with an inner diameter * outer diameter of 1 * 1.4 mm was selected for the subsequent degradation experiments. Fig. 4c shows the UV absorption spectra of tetracycline treated with ultrasonic for different times. The control group used a glass tube with the same diameter of PTFE capillary tube. As the reaction time increases, the intensity of the characteristic absorption peak of tetracycline at 357 nm decreases. The results of percentage degradation of tetracycline with reaction time show that the degradation of tetracycline increases significantly as the reaction time increases, while the tetracycline in the control group is little degraded (Fig. 4d). We also investigated the degradation of tetracycline with different concentrations (5, 10, 15, 20 μg mL^{-1}), and tetracycline with the concentration of 5 μg mL^{-1} was degraded completely after treated for 60 min (Fig. 4e). The degradation of tetracycline at different pH show that the degradation rate increases gradually as the pH increases (Fig. 4 f). To understand the degradation mechanism, different free radical scavengers was added to the initial tetracycline solution. Tert-butanol, 1,4-Benzoquinone and $AgNO_3$ were used as scavenger for hydroxyl radical, superoxide anion radical and electron, respectively. As indicated in Fig. 4 g, the removal efficiency of tetracycline is about 59% without the addition of the radical scavengers. When $AgNO_3$ was added, there was no significant change in tetracycline degradation. However, when tert-butanol and 1,4-Benzoquinone are used, the degradation processes are significantly inhibited, and the corresponding removal efficiencies decrease to about 13% and 38%, respectively. Therefore,·OH and·O_2^- are predominant reactive species for the oxidative degradation of tetracycline, and the influence order of active species is·OH > ·O_2^-. In order to further understand the degradation mechanism, the product in solutions with different reaction time were measured using liquid chromatography-mass spectrometry (LC-MS). Fig. 4 h depicts the total ion flow chromatogram for different treatment times. The dominant peak at a retention time of 1.6 min with

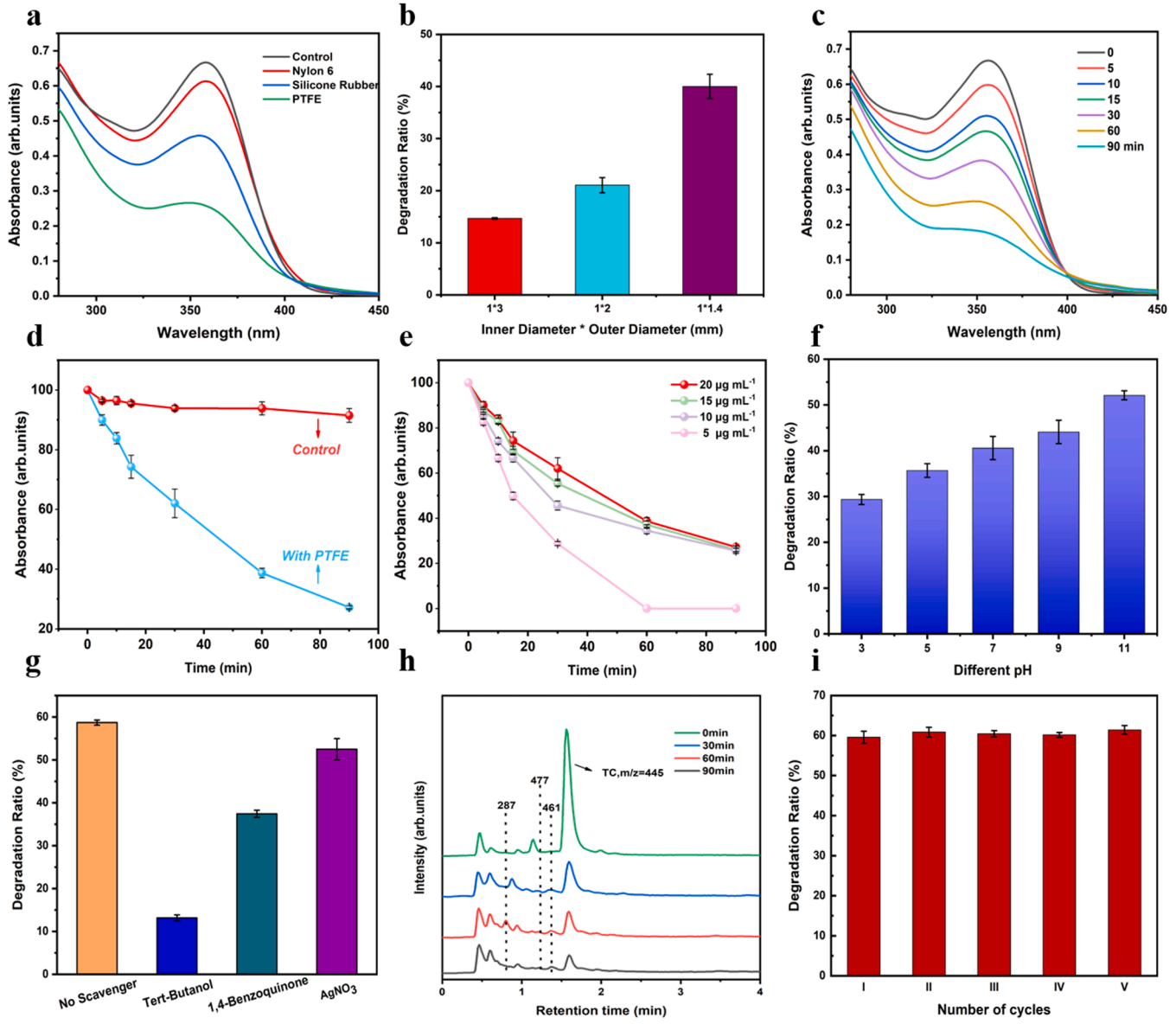

Fig. 4. Degradation of tetracycline. (a) Absorption spectra of 20 μg mL^{-1} tetracycline solution treated with different capillary tube materials (PTFE, Silicone Rubber, Nylon 6). (b) Maximum absorption of PTFE-treated 20 μg mL^{-1} tetracycline solution treated with different tube wall thickness (inner diameter*outer diameter: 1 *3 mm, 1 *2 mm, 1 *1.4 mm). (c) Absorption spectra of 20 μg mL^{-1} tetracycline solution treated with different times. (d) Degradation percentage curve of 20 μg mL^{-1} tetracycline solution treated with PTFE or glass tube with time. (e) Percentage degradation curves with time for different initial concentrations of tetracycline solution (f) Maximum absorption of 20 μg mL^{-1} tetracycline solution treated with PTFE capillary tube at different pH. (g) Maximum absorption of 20 μg mL^{-1} tetracycline solution treated with PTFE capillary tube by adding different free radical scavengers. (h) Total ion flow chromatograms of tetracycline solutions after treatment for different time periods. (i) Maximum absorption of 20 μg mL^{-1} tetracycline solution treated with PTFE capillary tube after replicate cycles. Error bars represent standard deviation based on three replicate data.

an *m/z* of 445 corresponds to tetracycline. As the reaction time prolonged, the intensity of the main peak gradually decreases with the appearance of other peaks. The corresponding possible degradation products were presented in the detailed analysis of the mass spectra (Fig. S9 and Table S1). Fig. S10 proposes the possible degradation pathways of tetracycline. The stability of the degradation system was also investigated. As shown in Fig. 4i, the degradation efficiency remains the same after five replicate cycles.

4. Conclusions

In summary, we developed a highly sensitive strategy based on a long capillary tube to investigate the electron transfer and free radical generation during solid-liquid contact. In this strategy, a small droplet was pushed through a long capillary tube by nitrogen gas flow and the droplet was collected for the analysis of free radical generation. This strategy has the following advantages: (1) it can produce a large solid-liquid contact interface for a small volume of water; (2) the free radical concentration can be increased by extending the tube length; (3) oxygen interference can be eliminated by the nitrogen atmosphere. Base on this strategy,·OH radicals generated by contact electrification at solid-liquid interface without any additional energy assistance (such as ultrasonic) are successfully detected. The mechanism investigation suggesting that·OH was generated from OH^- in water by losing one electron when it contacted with solid layer such as PTFE. Notably,·O_2^- was not detected in the solid-liquid contact process. When an ultrasonic is applied, both·OH and·O_2^- were generated. Furthermore, the generated free radicals were applied to degrade tetracycline pollution. This work

provides a new insight of the free radical generation during solid-liquid contact.

CRediT authorship contribution statement

Yi Zhao: Investigation, Formal analysis. Visualization, Writing – original draft. **Yang Liu:** Investigation, Writing – review & editing. **Yuying Wang:** Investigation, Writing – review & editing. **Shulan Li:** Investigation. **Yi Liu:** Conceptualization ideas, Writing – review & editing, Supervision, Project administration. **Zhong Lin Wang:** Conceptualization ideas, Writing – review & editing, Supervision, Project administration. **Peng Jiang:** Conceptualization ideas, Writing – review & editing, Supervision, Project administration.

Declaration of Competing Interest

The authors declare that they have no known competing financial interests or personal relationships that could have appeared to influence the work reported in this paper.

Data Availability

Data will be made available on request.

Acknowledgements

This research was supported by the National Natural Science Foundation of China (22074113, 22073070), the Young Top-notch Talent Cultivation Program of Hubei Province, Science and Technology Plans of Tianjin (22ZYJDSS00070, 21JCQNJC01470), and the Large-scale Instrument and Equipment Sharing Foundation of Wuhan University (LF20221381).

Appendix A. Supporting information

Supplementary data associated with this article can be found in the online version at doi:10.1016/j.nanoen.2023.108464.

References

[1] Q.L. Wen, J.Y. Duan, W.B. Wang, D.J. Huang, Y.W. Liu, Y.L. Shi, J.K. Fang, A. Nie, H.Q. Li, T.Y. Zhai, Engineering a local free water enriched microenvironment for surpassing platinum hydrogen evolution activity, Angew. Chem. Int. Ed. Engl. 61 (2022), e202206077.
[2] K. Du, L.F. Zhang, J.Q. Shan, J.X. Guo, J. Mao, C.C. Yang, C.H. Wang, Z.P. Hu, T. Ling, Interface engineering breaks both stability and activity limits of RuO_2 for sustainable water oxidation, Nat. Commun. 13 (2022) 5448.
[3] K.A. Sun, X.Y. Wu, Z.W. Zhuang, L.Y. Liu, J.J. Fang, L.Y. Zeng, J.G. Ma, S.J. Liu, J. Z. Li, R.Y. Dai, X. Tan, K. Yu, D. Liu, W.C. Cheong, A.J. Huang, Y.Q. Liu, Y. Pan, H. Xiao, C. Chen, Interfacial water engineering boosts neutral water reduction, Nat. Commun. 13 (2022) 6260.
[4] X.J. Zhao, S.Y. Kuang, Z.L. Wang, G. Zhu, Electricity-free electroluminescence excited by droplet impact driven triboelectric field on solid-liquid interface, Nano Energy 75 (2020), 104823.
[5] J.Y. Liu, Z. Wen, H. Lei, Z.Q. Gao, X.H. Sun, A liquid-solid interface-based triboelectric tactile sensor with ultrahigh sensitivity of 21.48 kPa^{-1}, Nano-Micro Lett. 14 (2022) 88.
[6] J. Chen, H.Y. Guo, J.G. Zheng, Y.Z. Huang, G.L. Liu, C.G. Hu, Z.L. Wang, Self-powered triboelectric micro liquid/gas flow sensor for microfluidics, ACS Nano 10 (2016) 8104–8112.
[7] X.Q. Zhang, M. Yu, Z. Ma, H.O. Yang, Y. Zou, S.L. Zhang, H.K. Niu, X.X. Pan, M. Y. Xu, Z. Li, Z.L. Wang, Self-powered distributed water level sensors based on liquid-solid triboelectric nanogenerators for ship draft detecting, Adv. Funct. Mater. 29 (2019) 1900327.
[8] J.T. Hu, W.J. Ren, X. Chen, Y.W. Li, W.Y. Huang, K. Yang, L.Y. Yang, Y. Lin, J. X. Zheng, F. Pan, The role of anions on the Helmholtz Plane for the solid-liquid interface in aqueous rechargeable lithium batteries, Nano Energy 74 (2020), 104864.
[9] L. Suo, B. Oleg, T. Gao, O. Marco, J. Ho, X. Fan, C. Luo, C. Wang, K. Xu, "Water-in-salt" electrolyte enables high-voltage aqueous lithium-ion chemistries, Science 350 (2015) 938–943.
[10] I.I. Nedrygailov, C. Lee, S.Y. Moon, H. Lee, J.Y. Park, Hot electrons at solid-liquid interfaces: a large chemoelectric effect during the catalytic decomposition of hydrogen peroxide, Angew. Chem. Int. Ed. Engl. 55 (2016) 10859–10862.
[11] C. Yan, H.R. Li, X. Chen, X.Q. Zhang, X.B. Cheng, R. Xu, J.Q. Huang, Q. Zhang, Regulating the inner Helmholtz Plane for stable solid electrolyte interphase on lithium metal anodes, J. Am. Chem. Soc. 141 (2019) 9422–9429.
[12] J.K. Lee, H.S. Han, S. Chaikasetsin, D.P. Marron, R.M. Waymouth, F.B. Prinz, R.N. Zare, Condensing water vapor to droplets generates hydrogen peroxide, Proc. Natl. Acad. Sci. U.S.A. 117 (2020) 30934–30941.
[13] C. Xu, Y.L. Zi, A.C. Wang, H.Y. Zou, Y.J. Dai, X. He, P.H. Wang, Y.C. Wang, P. Z. Feng, D.W. Li, Z.L. Wang, On the electron-transfer mechanism in the contact-electrification effect, Adv. Mater. 30 (2018), e1706790.
[14] S.Q. Lin, L. Xu, L.P. Zhu, X.Y. Chen, Z.L. Wang, Electron transfer in nanoscale contact electrification: photon excitation effect, Adv. Mater. 31 (2019), e1901418.
[15] C. Xu, A.C. Wang, H.Y. Zou, B.B. Zhang, C.L. Zhang, Y.L. Zi, L. Pan, P.H. Wang, P. Z. Feng, Z.Q. Lin, Z.L. Wang, Raising the working temperature of a triboelectric nanogenerator by quenching down electron thermionic emission in contact-electrification, Adv. Mater. 30 (2018), e1803968.
[16] S.Q. Lin, L. Xu, C. Xu, X.Y. Chen, A.C. Wang, B.B. Zhang, P. Lin, Y. Yang, H.B. Zhao, Z.L. Wang, Electron transfer in nanoscale contact electrification: effect of temperature in the metal-dielectric case, Adv. Mater. 31 (2019), e1808197.
[17] Z.L. Wang, A.C. Wang, On the origin of contact-electrification, Mater. Today 30 (2019) 34–51.
[18] S.Q. Lin, L. Xu, A.C. Wang, Z.L. Wang, Quantifying electron-transfer in liquid-solid contact electrification and the formation of electric double-layer, Nat. Commun. 11 (2020) 399.
[19] J.H. Nie, Z.W. Ren, L. Xu, S.Q. Lin, F. Zhan, X.Y. Chen, Z.L. Wang, Probing contact-electrification-induced electron and ion transfers at a liquid-solid interface, Adv. Mater. 32 (2020), e1905696.
[20] Z.M. Wang, A. Berbille, Y.W. Feng, S. Li, L.P. Zhu, W. Tang, Z.L. Wang, Contact-electro-catalysis for the degradation of organic pollutants using pristine dielectric powders, Nat. Commun. 13 (2022) 130.
[21] L.M. Jiang, Y. Yang, Y. Chen, Q.F. Zhou, Ultrasound-induced wireless energy harvesting: from materials strategies to functional applications, Nano Energy 77 (2020), 105131.
[22] K. Yasui., Acoustic cavitation and bubble dynamics, Springer International Publishing, Berlin, 2017.
[23] Z.L. Wang, L. Lin, J. Chen, S.M. Niu, Y.L. Zi, eds., Triboelectric nanogenerators, Springer International Publishing, Berlin, 2016.
[24] H.Y. Zou, Y. Zhang, L.T. Guo, P.H. Wang, X. He, G.Z. Dai, H.W. Zheng, C.Y. Chen, A.C. Wang, C. Xu, Z.L. Wang, Quantifying the triboelectric series, Nat. Commun. 10 (2019) 1427.
[25] S.Y. Du, J.S. Francisco, S. Kais, Study of electronic structure and dynamics of interacting free radicals influenced by water, J. Chem. Phys. 130 (2009), 124312.
[26] P. Jiang, L. Zhang, H.Y. Guo, C.Y. Chen, C.S. Wu, S. Zhang, Z.L. Wang, Signal output of triboelectric nanogenerator at oil-water-solid multiphase interfaces and its application for dual-signal chemical sensing, Adv. Mater. 31 (2019), e1902793.
[27] M. Hayyan, M.A. Hashim, I.M. AlNashef, Superoxide ion: generation and chemical implications, Chem. Rev. 116 (2016) 3029–3085.
[28] Y.Z. Hong, C.S. Li, B.X. Yin, D. Li, Z.Y. Zhang, B.D. Mao, W.Q. Fan, W. Gu, W. D. Shi, Promoting visible-light-induced photocatalytic degradation of tetracycline by an efficient and stable beta-Bi_2O_3@g-C_3N_4 core/shell nanocomposite, Chem. Eng. J. 338 (2018) 137–146.
[29] S. Leong, D. Li, K. Hapgood, X. Zhang, H. Wang, $Ni(OH)_2$ decorated rutile TiO_2 for efficient removal of tetracycline from wastewater, Appl. Catal. B 198 (2016) 224–233.
[30] C.M. Li, S.Y. Yu, H.J. Dong, C.B. Liu, H.J. Wu, H.N. Che, G. Chen, Z-scheme mesoporous photocatalyst constructed by modification of Sn_3O_4 nanoclusters on g-C_3N_4 nanosheets with improved photocatalytic performance and mechanism insight, Appl. Catal. B 238 (2018) 284–293.
[31] X.X. Zhao, Z.Y. Lu, M.B. Wei, M.H. Zhang, H.J. Dong, C.W. Yi, R. Ji, Y.S. Yan, Synergetic effect of carbon sphere derived from yeast with magnetism and cobalt oxide nanochains towards improving photodegradation activity for various pollutants, Appl. Catal. B 220 (2018) 137–147.
[32] Z. Zhu, P.W. Huo, Z. Lu, Y.S. Yan, Z. Liu, W.D. Shi, C.X. Li, H.J. Dong, Fabrication of magnetically recoverable photocatalysts using g-C_3N_4 for effective separation of charge carriers through like-Z-scheme mechanism with Fe_3O_4 mediator, Chem. Eng. J. 331 (2018) 615–625.

Yi Zhao received his BS degree from Liaoning University in 2020. Since then, he became a postgraduate in professor Yi Liu's laboratory at College of Chemistry and Molecular Sciences, Wuhan University. His research focuses on contact electrification at the solid-liquid interface and contact-electrocatalysis. and biological applications of nanomaterials.

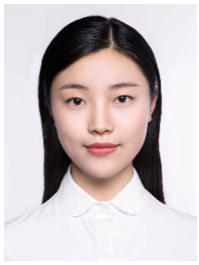

Yang Liu received her BS degree from Liaoning University in 2020. Since then, she became a postgraduate in professor Yi Liu's laboratory at College of Chemistry and Molecular Sciences, Wuhan University. Her research focuses on the anticancer application of hydroxyl radicals in cells and animals.

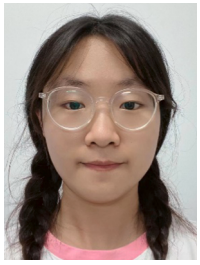

Yuying Wang recieved her BS degree from Wuhan University in 2019. She then became a doctoral student in professor Yi Liu's laboratory at College of Chemistry and Molecular Sciences, Wuhan University. Her current research focuses on the synthesis and biological applications of nanozymes.

Shulan Li received her Ph.D. degree from Wuhan University in 2021. She is currently an associate professor at College of Chemistry, Tiangong University. Her research interests include anticancer and antibacterial therapy of nanomaterials.

Yi Liu graduated from the Department of Chemistry at Wuhan University where, he also concluded his B. Sc., M.Sc. and Ph.D. programs. He is currently a distinguished professor at the College of Chemistry and Molecular Sciences at Wuhan University and vice president of Tiangong University. His research focuses on the synthesis, biological effect and application of nanomaterials, and multifunctional molecular probes.

Zhong Lin Wang received his Ph.D. degree from Arizona State University in physics. He now is the Hightower Chair in Materials Science and Engineering, Regents' Professor at Georgia Tech, the chief scientist and director of the Beijing Institute of Nanoenergy and Nanosystems, Chinese Academy of Sciences. Prof. Wang has made original and innovative contributions to the synthesis, discovery, characterization and understanding of fundamental physical properties of oxide nanobelts and nanowires, as well as applications of nanowires in energy sciences, electronics, optoelectronics and biological science. His discovery and breakthroughs in developing nanogenerators establish the principle and technological road map for harvesting mechanical energy from environmental and biological systems for powering personal electronics. His research on self-powered nanosystems has inspired the worldwide efforts in academia and industry for studying energy for micro-nano-systems, which is now a distinct disciplinary in energy research and future sensor networks. He coined and pioneered the fields of piezotronics and piezophototronics by introducing piezoelectric potential gated charge transport process in fabricating new electronic and optoelectronic devices.

Peng Jiang received his Ph.D. degree (2013) from Wuhan University. Currently, he is an associate professor at School of Pharmaceutical Sciences, Wuhan University. He worked as a visiting scholar in Prof. Zhonglin Wang's group at Georgia Institute of Technology in 2017–2019. His research interests include fluorescent nanomaterials, theranostic nanomaterials, and self-powered functional nanodevice.